Title
REACTIONS OF CHLORINE WITH LIQUID METALS -II LEAD

Authors
Balooch, M.
Siekhaus, W.J.
Olander, D.R.

Publication Date
1983-07-01

Lawrence Berkeley Laboratory
UNIVERSITY OF CALIFORNIA

Materials & Molecular Research Division

Submitted to the Journal of Physical Chemistry

REACTIONS OF CHLORINE WITH LIQUID METALS - II LEAD

M. Balooch, W.J. Siekhaus, and D.R. Olander

July 1983

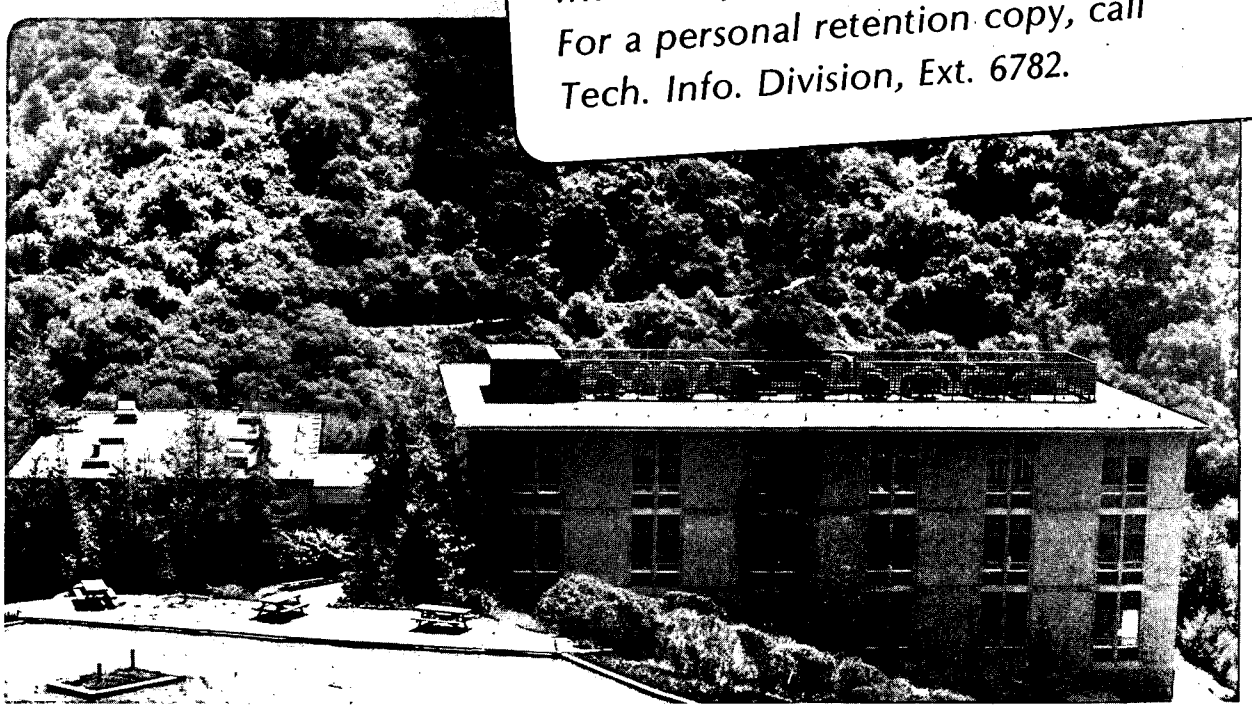

Prepared for the U.S. Department of Energy under Contract DE-AC03-76SF00098

DISCLAIMER

REACTIONS OF CHLORINE WITH LIQUID METALS - II LEAD

M. Balooch[+], W. J. Siekhaus[*] and D. R. Olander

This work was supported by the Director, Office of Energy Research, Office of Basic Energy Sciences, Materials Sciences Division of the U. S. Department of Energy under contract #DE-AC03-76SF00098 and the U. S. Department of Energy under contract No. W-7405-Eng-48, and by the U. S. Army Research Office, Research Triangle Park, North Carolina under contract No. 15812-MS.

[+]Materials and Molecular Research Division of the Lawrence Berkeley Laboratory and the Department of Nuclear Engineering, University of California, Berkeley, California 94720

[*]Chemistry Division of the Lawrence Livermore National Laboratory

A B S T R A C T

The reaction of molecular chlorine with solid and liquid lead surfaces was studied by modulated molecular beam-mass spectrometric methods in the temperature range 300-900K and at equivalent chlorine pressures between 5×10^{-6} and 5×10^{-4} Torr. The only detectable volatile reaction product was $PbCl_2$. Up to the melting point of lead (601K) the apparent reaction probability did not exceed 10^{-3}. For the liquid phase, production of $PbCl_2$ increased rapidly with increasing surface temperature and the reaction was nonlinear with respect to chlorine equivalent pressure. A reaction model was developed which takes into account solution-diffusion of chlorine from the surface into the liquid and production of $PbCl_2$ by parallel Eley-Rideal and Langmuir Hinshelwood mechanisms.

I INTRODUCTION

The present work is a continuation of the gas-liquid reaction studies initiated in Part I(1). The investigation is based on the modulated molecular beam technique utilizing phase-sensitive detection of reaction products by an in-situ mass spectrometer. The surface is monitored by AES in a separate chamber simulating the experimental conditions of the molecular beam chamber. Details of the experimental method and data analysis procedures are given in Ref. 1.

In Part I, the rate of the indium-chlorine reaction was found to increase sharply at or just below the melting point of the metal. Auger electron spectroscopy of the reacting surface showed an equally sharp decrease in the surface chlorine concentration over approximately the same temperature range. In the present study, particular attention is paid to the reaction of chlorine with the liquid phase of lead. The reaction is compared with the results of the In-Cl_2 study(1) as well as with those from a molecular beam investigation of the Fe-Cl_2 reaction(2).

II. RESULTS

The lead-containing ions observed in the mass spectrometer are $PbCl_2^+$, $PbCl^+$ and Pb^+. All have the same phase angle and the same dependence on surface temperature, which strongly suggests that the sole volatile product of reaction is $PbCl_2$.

Figure 1 shows the measured reaction probability ε and the conjugate phase lag ϕ for the volatile $PbCl_2$ product as functions of surface temperature. The apparent reaction probability observed for the solid

phase of lead is smaller than 10^{-3}, which is approximately the limit of detection of the mass spectrometer for this species. Therefore quantitative experimental information could not be obtained in this region. However, a distinct increase in ε is observed at the melting point, although the jump is not as abrupt as it was for indium(1). The reactivity continues to increase rapidly with temperature up to 900 K, at which point the vapor pressure of lead prevents exploration of higher temperatures. The phase lag does not change monotonically with temperature but rather goes through a maximum of $\sim$ 800 K, which suggests a branched process(3,4).

The nonlinearity of the reaction is clear from the beam-intensity dependence of the reaction product amplitude and phase(Fig. 2). The phase lag decreases with beam intensity beyond $\sim 1.5 \times 10^{16}$ molecules/cm^2-s, below which it remains almost constant at about 41°. This behavior indicates bulk diffusion control at low beam intensities(3,4).

The frequency dependences of the apparent reaction probability and phase lag are shown in Fig. 3 for constant temperature and beam intensity. The phase lag increases with frequency up to $\sim$ 100 Hz and appears to level off thereafter at $\sim 42^{\circ}$ which is another manifestation of diffusion control of the process.

The surface coverage of chlorine as a function of temperature at a Cl_2 impingement rate of 5.5×10^{16} molecules/cm^2-s (obtained in the AES chamber) is shown in Fig. 4. It appears that the surface is saturated with chlorine up to $\sim$ 450K, after which a drastic decrease with increasing temperature occurs. In the temperature range of the liquid reactant (> 600K), the chlorine concentration on the surface is less than 10% of the saturation value.

III. REACTION MODEL FOR LIQUID LEAD

The following reaction model is based upon several salient features of the experimental results, namely, the nonlinearity of the reaction, the probable existence of a branch process and diffusion into the liquid. Dissociative chemisorption of molecular chlorine takes place with a sticking probability η on the surface of the bare liquid exposed to the impinging reactant beam,

$$Cl_2(g) \xrightarrow{\eta} 2\ Cl(ads) \qquad (1)$$

The remaining elementary reaction steps are

$$Cl(ads) \underset{}{\overset{H,D}{\rightleftharpoons}} Cl(soln) \qquad (2)$$

$$Pb(\ell) + Cl(ads) \overset{K}{\rightleftharpoons} PbCl(ads) \qquad (3)$$

$$PbCl(ads) \xrightarrow{k_{LH}} PbCl_2(g) \qquad (4)$$

$$PbCl(ads) + Cl_2(g) \xrightarrow{\eta_{ER}} PbCl_2(g) + Cl(ads) \qquad (5)$$

Reaction(2) represents dissolution with solubility coefficient H and migration with diffusivity D of chlorine atoms into the liquid. Reaction (3) denotes equilibrium between adsorbed chlorine and lead monochloride. The production and desorption of $PbCl_2$ through a Langmuir-HInshelwood branch is shown in step (4) with rate constant k_{LH}. Reaction (5) is the Eley-Rideal branch which provides the second pathway for production of $PbCl_2$. It is characterized by a reactive sticking probability denoted by η_{ER}.

The balance on chlorine adsorbed on the liquid lead surface as either Cl(ads) or PbCl(ads) is:

$$(1 + K)\frac{dn}{dt} = 2\eta I_o g(t) - 2Kk_{LH}n^2 + D\left(\frac{\partial c}{\partial z}\right)_{z=0} \qquad (6)$$

where n is the Cl(ads) concentration. According to Eq.(3), the concentration of PbCl(ads) is Kn. Depth into the liquid is denoted by z.

The first term on the right hand side of Eq.(6) represents the source of surface Cl atoms from dissociative chemisorption of incident Cl_2 molecules. Because the surface chlorine concentration above 600K has been shown by AES to be low, the coverages of Cl(ads) and PbCl(ads) are assumed to be small and the presence of these species does not affect sticking of Cl_2. The second term is the loss due to production of $PbCl_2$ by the Langmuir-Hinshelwood route at a rate $R_{LH} = Kk_{LH}n^2$.

The rate of $PbCl_2$ production by the Eley-Rideal mechanism is expressed by:

$$R_{ER} = \eta_{ER}\left(\frac{Kn}{N_s}\right) I_o g(t) \qquad (7)$$

where the quantity in parentheses is the fractional coverage of the surface by PbCl. The site density on the surface is N_s cm^{-2}. The E-R term does not appear in Eq.(6) because reaction (5) merely replaces PbCl(ads) by Cl(ads), resulting in no net change in total surface chlorine. The quantity η_{ER} is the probability of reaction when an incident Cl_2 molecule strikes an adsorbed PbCl species.

The last term in Eq(6) represents the loss of chlorine atoms from the surface by solution and diffusion into the liquid metal in which the concentration of chlorine is denoted by c. The diffusion process is governed by Fick's law applied to a semi-infinite medium:

$$\frac{\partial c}{\partial t} = D\frac{\partial^2 c}{\partial z^2} \qquad (8)$$

The surface boundary condition for this equation, which links the bulk diffusion process to the surface reactions governed by Eq(6), assumes physical distribution of Cl between the adsorbed state and the liquid metal at the surface:

$$c(z=0) = Hn \tag{9}$$

where H is the distribution coefficient for the surface-bulk partitioning of chlorine.

Simultaneous solution of Eqs(6), (8), and (9) is accomplished by the Fourier expansion method outlined in Ref. 1. The model predictions are contained in the reaction product vector, which is the ratio of the fundamental mode of the product emission rate ($R_{LH} + R_{ER}$) to that of the incident beam impingement rate [$I_o g(t)$]. The scaler components of the reaction product vector are the apparent reaction probability and the phase lag. They are given by:

$$\phi = \tan^{-1}\left\{\frac{2\pi f + \sqrt{\pi H^2 Df}}{\sqrt{4\eta I_o K k_{LH}} + \sqrt{\pi H^2 Df} + \frac{1}{F}\left(\frac{K\eta_{ER}}{N_s}\right)\sqrt{\frac{\eta I_o}{2k_{LH}K}}}\right\} \tag{10}$$

$$\varepsilon = \frac{\left(\sqrt{4\eta I_o K k_{LH}} + \sqrt{\pi H^2 Df}\right)F + \left(\frac{K\eta_{ER}}{N_s}\right)\sqrt{\frac{\eta I_o}{2k_{LH}K}}}{\cos\phi} \tag{11}$$

where:

$$F = \eta\,\frac{\sqrt{8\eta I_o K k_{LH}} + \left(\frac{K\eta_{ER}}{N_s}\right)I_o}{\left(\sqrt{4\eta I_o K k_{LH}} + \sqrt{\pi H^2 Df}\right)^2 + \left(2\pi f + \sqrt{\pi H^2 Df}\right)^2} \tag{12}$$

The explicit dependences of ε and ϕ on the experimental variables I_o and f are seen in these formulas. The temperature appears implicitly in

the rate constants. In addition, four parameters of the reaction model appear in Eqs.(10) - (12). These are the sticking probability η, the parameter characterizing the Langmuir-Hinshelwood step, Kk_{LH}, the comparable parameter for the direct reaction, $K\eta_{ER}/N_S$, and the solution-diffusion parameter H^2D. The values of these parameters and their temperature dependences which provide the best agreement between model and experiment are determined by a type of least-squares computation modified to accommodate complex numbers (i.e., the ε-ϕ conjugate pairs). The results of the fitting process are shown in Table 1 and comparisons of Eqs.(10) and (11) with the data are shown as the solid curves in Figs. 1 - 3. Equation (10) shows that the maximum in the phase lag vs. temperature plot (Fig. 1) is due to the interplay of both the L-H and E-R surface reactions and bulk diffusion. The strong nonlinearity displayed by Fig. 2 is reflected in the appearance of the beam intensity I_o in the denominator of Eq(10) (which causes ϕ to decrease as I_o increases) and in the numerator of Eq(11), which results in the opposite trend for ε. At high modulation frequencies, the solution-diffusion term in the denominator of Eq(10) is larger than the other two. Because H^2D is large, this term dominates the $2\pi f$ term in the numerator as well. Thus, the argument of the arc tangent is near unity, and the phase lag approaches 45^o as seen in Fig. 3.

The reaction model also provides the following result for the total surface chlorine concentration when the liquid is exposed to a steady beam of intensity I:

$$(Cl + PbCl)_{ads} = (1+K)\left(\frac{\eta I}{Kk_{LH}}\right)^{\frac{1}{2}} \quad (atoms/cm^2) \qquad (13)$$

Dividing this quantity by the saturation concentration of $3x10^{14}$ cm^{-2},

as estimated for the In-Cl_2 reaction(1), and assuming $K << 1$, the theoretical coverage on the liquid is shown as the curve in Fig. 4 for $T > 600$ K. Argreement with the AES data could be improved by setting $K = 0.1$. Because the AES results were not used in determining the reaction parameters used in Eq(13), the good accord shown in Fig. 4 constitutes independent verification of the model.

IV. DISCUSSION

The sticking probability of Cl_2 on liquid lead ($\eta = 0.04$) is roughly twice that on liquid indium(1). However, unlike the latter metal, i.e., the Pb/Cl_2 reaction rate does not reach the reactant supply limit (i.e., when ε is temperature independent and $\phi = 0$) at the maximum attainable temperature of 900 K. In the In-Cl_2 reaction, the reaction product for the liquid metal is the monochloride, whereas in the case of liquid lead, only the dichloride is observed. The two liquid metals also differ in the way that the overlayer of metal chloride is destroyed at high temperature. In the case of indium, the InCl layer appears to desorb directly into the gas and to break up into islands on the liquid metal surface. The lead chloride layer, on the other hand, is removed by dissolving into the bulk liquid as well as by reaction to form volatile $PbCl_2$.

The reaction of lead with chlorine has several features in common with the corresponding reaction with iron(2). In both cases, the only volatile species is the dichloride, which is produced by parallel Langmuir-Hinshelwood and Eley-Rideal paths. The kinetics in the two cases are strongly influenced by solution and diffusion of chlorine in the bulk material. However, because iron is solid during the

experiments, diffusion occurs in a substoichiometric chloride scale which builds up on the substrate rather than directly into the metal, as is the case with lead. Another difference between the responses of iron and lead surfaces to chlorine molecular beams is the slow desorption rate of the dichloride observed in the former case. A consequence of this rate limitation is reduction of molecular chlorine adsorption due to partial coverage of the surface by reaction product. In the lead-chlorine system, on the other hand, product desorption appears to be rapid compared to the preceding steps in the mechanism and the kinetics are not coverage-dependent.

The activation energy for production of the dichloride via the Langmuir-Hinshelwood surface process is larger for iron (46 kcal/mole) than for lead (11 kcal/mole). This difference is not unexpected in view of the more refractory nature and stronger bonding in iron than in lead. The Eley-Rideal steps in the two reaction systems, on the other hand, are both virtually temperature-independent, although the magnitude of the direct reaction probability η_{ER} is much larger for lead than for the iron analog of Eq(5). According to Eq(7), η_{ER}/N_s is the cross section for reaction of an incident Cl_2 molecule and an adsorbed PbCl species. Using the value of $K\eta_{ER}/N_s$ given in Table 1 and taking $K \approx 0.1$ in accord with the preceding discussion of the AES data, the reactive cross section is calculated to be ~ 8 Å^2, which is not unreasonable. For $N_s = 3 \times 10^{14}$ cm^{-2}, the direct reaction probability of Cl_2 on PbCl is calculated to be $\eta_{ER} \approx 0.2$. Although this value is quite approximate due to the large uncertainties in the estimates of K and N_s, it is clearly considerably larger than the comparable quantity for iron ($\eta_{ER} < 0.002$).

The last noteworthy feature of the reaction characteristics collected in Table 1 is the negative activation energy of the solution diffusion parameter H^2D. This quantity is a type of permeability of the liquid metal to chlorine, inasmuch as it is the product of a solubility coefficient and a diffusivity. Since the latter represents a normally activated process with a positive activation energy, the negative activation energy for H^2D means that solution of surface-adsorbed chlorine by liquid lead is exothermic, so that the solubility coefficient H decreases as T increases more rapidly than D increases. Similar exothermic solution of hydrogen gas in niobium and vanadium is is well-known(5).

Acknowledgement

This work was supported by the Director, Office of Energy Research, Office of Basic Energy Sciences, Materials Sciences Division of the U. S. Department of Energy under contract #DE-AC03-76SF00098 and the U. S. Department of Energy under contract No. W-7405-Eng-48, and by the U. S. Army Research Office, Research Triangle Park, North Carolina under contract No. 15812-MS

REFERENCES

1. M. Balooch, W. J. Siekhaus and D. R. Olander, Part I of this series.

2. M. Balooch, W. J. Siekhaus and D. R. Olander, Trans. Farad. Soc., to be published.

3. R. H. Jones, D. R. Olander, W. J. Siekhaus and J. A. Schwarz, J. Vacuum Sci. Technol. 9, 1429 (1972).

4. J. A. Schwarz and R. J. Madix, Surface Sci. 46, 317 (1974).

5. R. E. Stickney, "The Chemistry of Fusion Technology," D. M. Gruen, Ed., Plenum Press (1972).

Table 1. Parameters of the $Pb(\ell)$-Cl_2 reaction

Parameter	Pre-exponential factor	Activation Energy (kcal/mole)
η	0.04	-
$K\, k_{LH}$	3.2×10^{-8} cm^2-s^{-1}	11
$\frac{K\, \eta_{ER}}{N_s}$	4×10^{-16} cm^2	2
H^2D	2.1×10^{2} s^{-1}	-10

FIGURE CAPTIONS

1. Apparent reaction probability and phase lag of $PbCl_2$ as a function of target temperature.
2. The effect of chlorine beam intensity on the apparent reaction probability and phase lag of $PbCl_2$ for constant temperature and chopping frequency.
3. Chopping frequency dependence of the apparent reaction probability and phase lag.
4. AES measurement of the temperature dependence of the surface chlorine coverage for fixed beam intensity of $\sim 5.5 \times 10^{16}$ molecules/cm^2-s. The solid line is deduced from the model with the contribution of PbCl(ads) neglected.

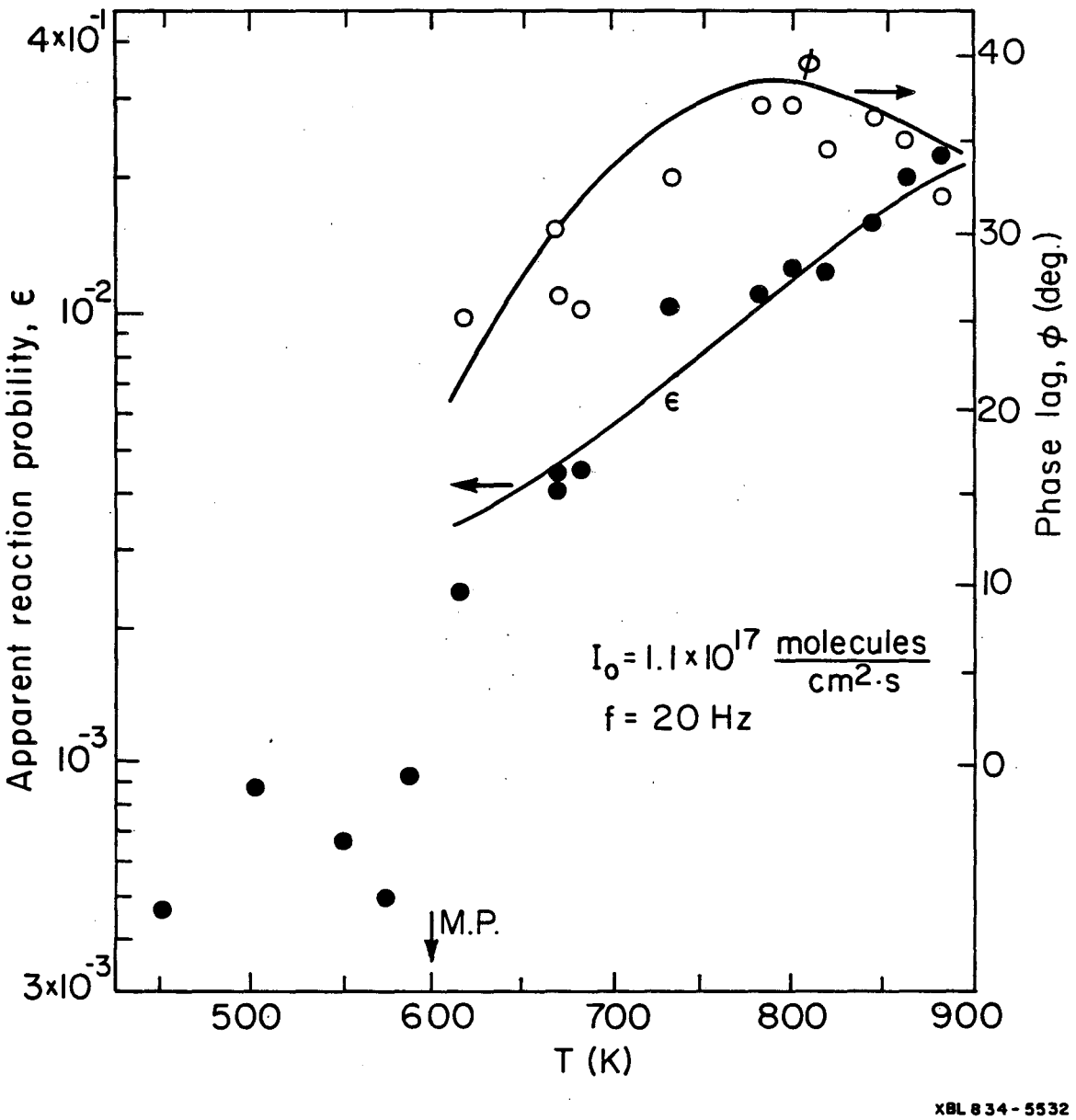
4x10⁻¹
10⁻²
10⁻³
3x10⁻³
Apparent reaction probility, ϵ
40
30
20
10
0
Phase lag, ϕ (deg.)
ϕ
ϵ
I₀ = 1.1 x 10¹⁷ molecules / cm²·s
f = 20 Hz
M.P.
500
600
700
800
900
T (K)
XBL 834-5532

Fig. 1

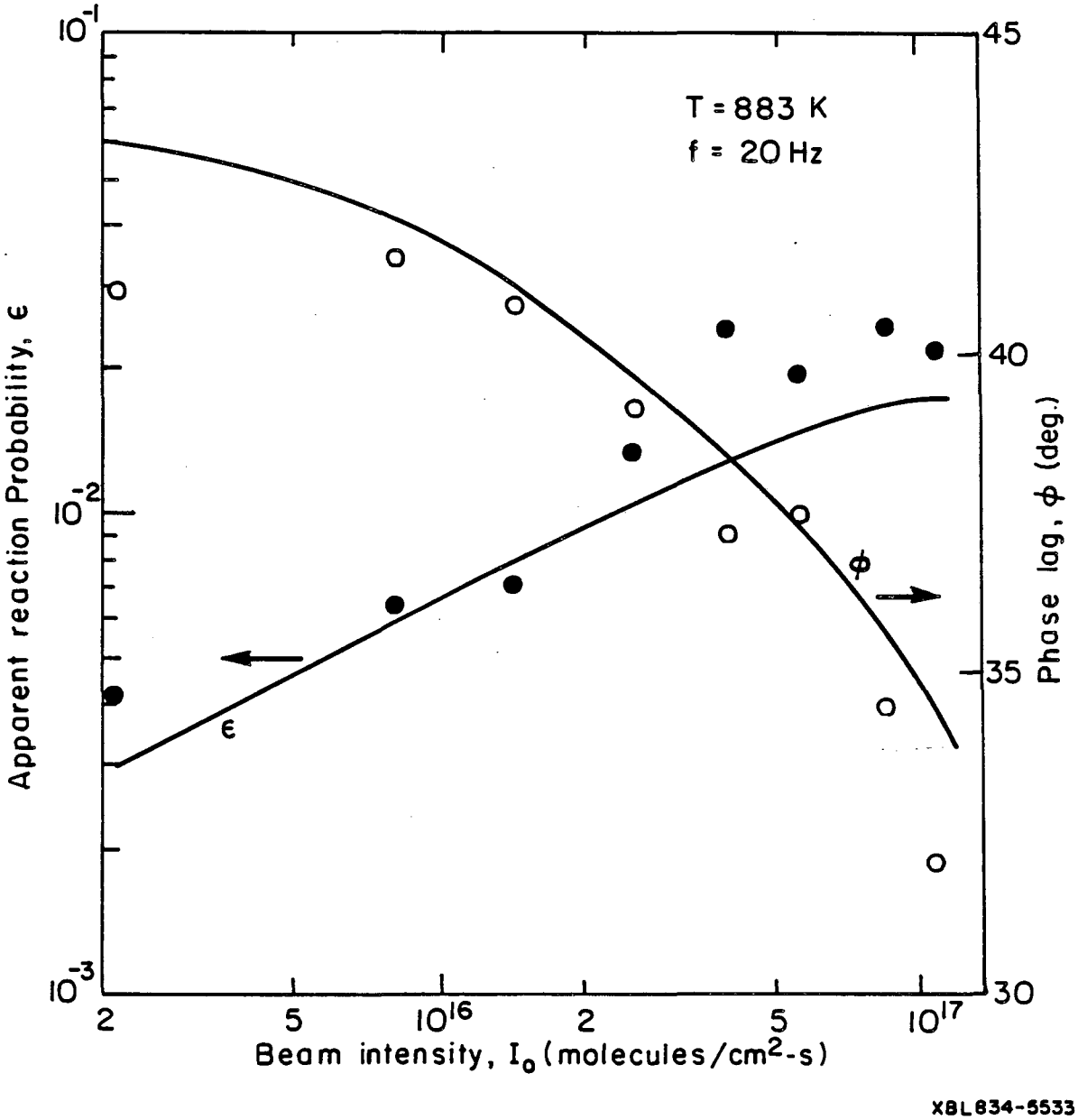
T = 883 K
f = 20 Hz
Apparent reaction Probability, ε
Phase lag, φ (deg.)
Beam intensity, I_0 (molecules/cm^2-s)
ε
φ
10^{-1}
10^{-2}
10^{-3}
45
40
35
30
2
5
10^{16}
2
5
10^{17}
XBL834-5533

Fig. 2

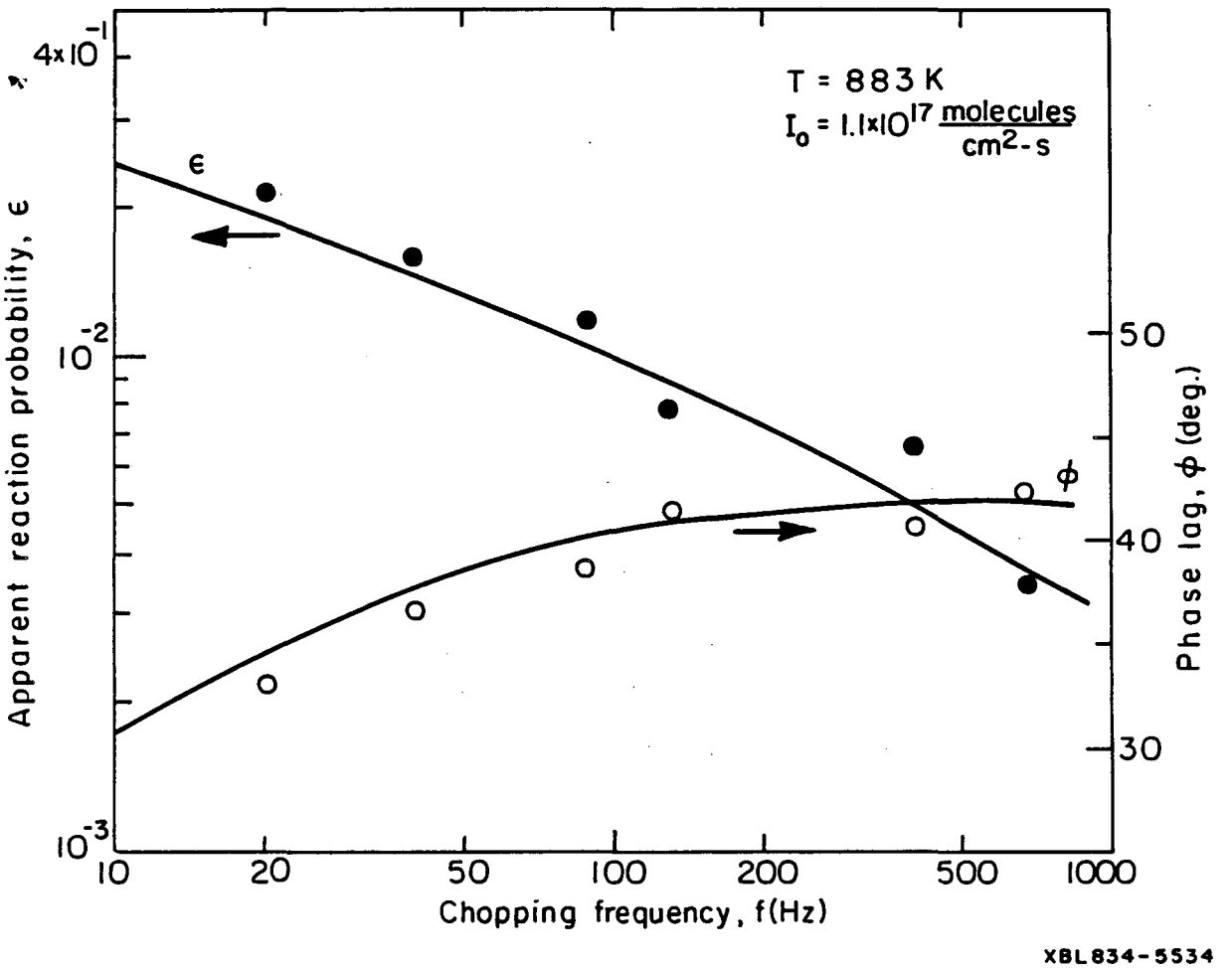
T = 883 K
I_o = 1.1x10^{17} molecules/cm^2-s
ε
φ
Apparent reaction probability, ε
Phase lag, φ (deg.)
Chopping frequency, f(Hz)
4x10^{-1}
10^{-2}
10^{-3}
10
20
50
100
200
500
1000
50
40
30
XBL834-5534

Fig. 3

TECHNICAL INFORMATION DEPARTMENT
LAWRENCE BERKELEY LABORATORY
UNIVERSITY OF CALIFORNIA
BERKELEY, CALIFORNIA 94720